Chapter 1

History of Solar Research

Naked-eye observations of sunspots go back for millenniums, and the first observations were done through smog or dust in order not to hurt one's eyesight. The first definite sunspot sighting was done in China in 165 BC. However, it was the invention of the telescope and Kepler's laws of planetary motion that really started solar research:

1610 Galileo Galilei observed dark spots on the solar surface with his telescope, and suspected them to be objects close to the surface of the solar globe. Since the Church at that time vigorously supported the idea that the sun is immaculate and blemish-free, Galileo was afraid to make his ideas public. For the next 230 years, sunspots were observed semi-regularly by several observers, but little progress was made in understanding their nature.

1715 The size of the solar disc was measured accurately during a solar eclipse.

1769 Prof. Alexander Wilson deduced that spots are depressions and the umbra of a sunspot shows the solid surface of the sun.

1794 Sir William Herschel reported his observations and suggested that there might be living beings inhabiting the solar interior.

1843 A sunspot cycle of about 10 years was discovered.

1851 The first photograph of a solar eclipse showed coronal structures and prominences.

1853 Richard Carrington, an amateur astronomer, determined solar rotation patterns.

1859 A solar flare was observed the first time, in white light.

1859 Gustav Kirchhoff found that the continuous spectrum produced by a hot solid body is transformed into a solar-like spectrum when light passes through a gas that is cooler than the solid.

1890s Solar surface temperature was derived to be around 6600 K, using the newly-discovered Stefan-Boltzmann law. Researchers generally assumed that the sun is made of gas.

1904 The connection between geomagnetic disturbances and sunspots was discovered.

1908 George Hale discovered solar magnetic fields with his polarization analyser, and found that sunspots have a bipolar character.

1926 A hydrodynamic model was developed to explain solar magnetic fields. It was later refined to a magnetohydrodynamic model.

1930s Speculation arose that the sun's energy source is nuclear. In 1939 it was proposed that the energy comes from the fusion of four hydrogen atoms.

1942 Solar radio emission was observed by the British Army radar operators.

1946 The intensity of the steady component of the solar radio emission, at different wavelengths, was explained by a 10 000 degree solar chromosphere (emitting at short wavelengths) and a million-degree solar corona (emitting at long wavelengths). It was predicted that the extremely hot solar corona would also emit in X-rays.

1949 Solar X-ray emission was observed during a rocket flight.

1958 It is proposed that the generator of solar magnetic fields is a dynamo, working inside the sun.

1958 The existence of a solar wind was predicted, and it was first observed a few years later.

1960 Solar oscillations were observed. The most typical period is 5 minutes, although many other periods exist as well. Seismic activity, with pressure modes and gravity modes, was suggested to be the explanation.

1960 Propagating shock fronts were observed on the solar disk in association with flare eruptions. These chromospheric signatures were later named Moreton waves, and they were explained as blast waves created in the flare processes.

1961 The 11-year sunspot cycle was explained to be a 22-year magnetic cycle. The model developed by Horace Babcock also explained the observed differential (non-uniform) solar rotation.

1964 The neutrino problem was discovered: there are less detected neutrinos than predicted by stellar models. Was this an observational problem or were the models based on fusion completely wrong?

1966 The first models where solar flares are explained to be the result of magnetic reconnection were developed.

1972 Solar gamma-ray emission was first observed.

1981 A detailed model of the solar atmosphere was published.

1981 Nano-flares were detected with new sensitive instruments and they were proposed to be the cause of coronal heating. It was later calculated that the total energy released in nanoflares is not sufficient to heat the corona, but people still searched for even smaller events (piko-flares etc.) that might go undetected because of the limits in instrument sensitivity.

1980's MHD (magnetohydrodynamic) models were developed to explain coronal heating.

1989 An intense solar flare caused geomagnetic storms that disrupted electric power transmission in Canada and put 6 million people without electricity for 9 hours. The term "space weather" was invented, to understand and predict how and when solar eruptions occur.

1994-95 The equatorial slow-speed solar wind and the fast polar region wind were detected in satellite observations. Large-scale polar coronal holes were also observed at that time.

1999 "EIT-waves" were discovered in EUV satellite observations. It was soon discovered that they were different from the earlier-observed Moreton waves, but it was still unclear if EIT waves were associated with flares or coronal mass ejections (CMEs), or both. Shock waves became a hot topic in solar physics.

2001 The neutrino-problem was resolved: not all neutrinos can be detected as they can oscillate and change their type on their way from the sun's interior to the earth.

2001 Sunspots on the backside of the sun were observed with holography techniques.

Solar physics entered a new era with the launch of the first spin-stabilized solar satellite in 1962 (Orbiting Solar Observatory, OSO-1). Its objective was to measure the solar electromagnetic radiation in the UV, X-ray, and gamma-ray regions. The solar observatory onboard the U.S. space station Skylab (launched in 1973), took the first full-disk X-ray images of the sun.

The GOES satellites (the first GOES-1 launched in 1975; latest GOES-13 launched in 2006) are a key element in United States' National Weather Service operations and they provide, for example, continuous observations of the solar X-ray flux. SMM (1980-1989) ja CGRO (1991-2000) provided solar data especially in hard X-rays and gamma-rays. The Japanese solar satellite Yohkoh (1991 – 2001) combined high-resolution soft and hard X-ray imaging with spectral information, and the satellite was operational for a decade.

SOHO was launched in 1995, and with its 12 different instruments it remains the largest and most expensive solar satellite so far. TRACE (1998-) is a Small Explorer (SMEX) mission, to image the solar corona and transition region at high angular and temporal resolution, mainly in EUV. Another SMEX mission, RHESSI (2002-), is the first instrument that can image solar flares in gamma-rays. The Japanese Hinode (launched in 2006) is carrying three advanced solar telescopes: one to observe solar magnetic fields with 0.2 arc sec resolution, one to image in X-rays with a resolution three times as high as Yohkoh, and one to get imaging and spectral information in EUV with a sensitivity ten times as high as SOHO. The imaging instruments of the Solar Dynamics Observatory (launched in 2010) have better spatial resolution and far better image cadence compared to SOHO, but otherwise similar performance. Solar Orbiter (launch scheduled around 2015 or later) will be one of the main future solar missions.

Although the solar cycle shows periods of low activity, the Sun is never really "quiet". Magnetic activity and plasma flows create structures and features that can be considered signs of activity at all times, e.g., sunspots and active regions, surges, plages, plumes, spicula, facula, moss and crinkles, bright points, radio brightenings, filaments, prominences, coronal holes, and solar wind. During activity maximum, spectacular large-scale features like flares, coronal mass ejections, filament eruptions, shock waves (Moreton waves, EIT-waves, SXT waves, etc.) and dimmings (EIT, SXT, radio, etc.) may appear daily.

Chapters 1 – 6 of these lecture notes give the basics of the structure of our nearest star, explain the radiation mechanisms that can be present, and describe the instruments that can be used in the observations. In Chapters 7 – 10 some of the observed features are discussed in more detail.

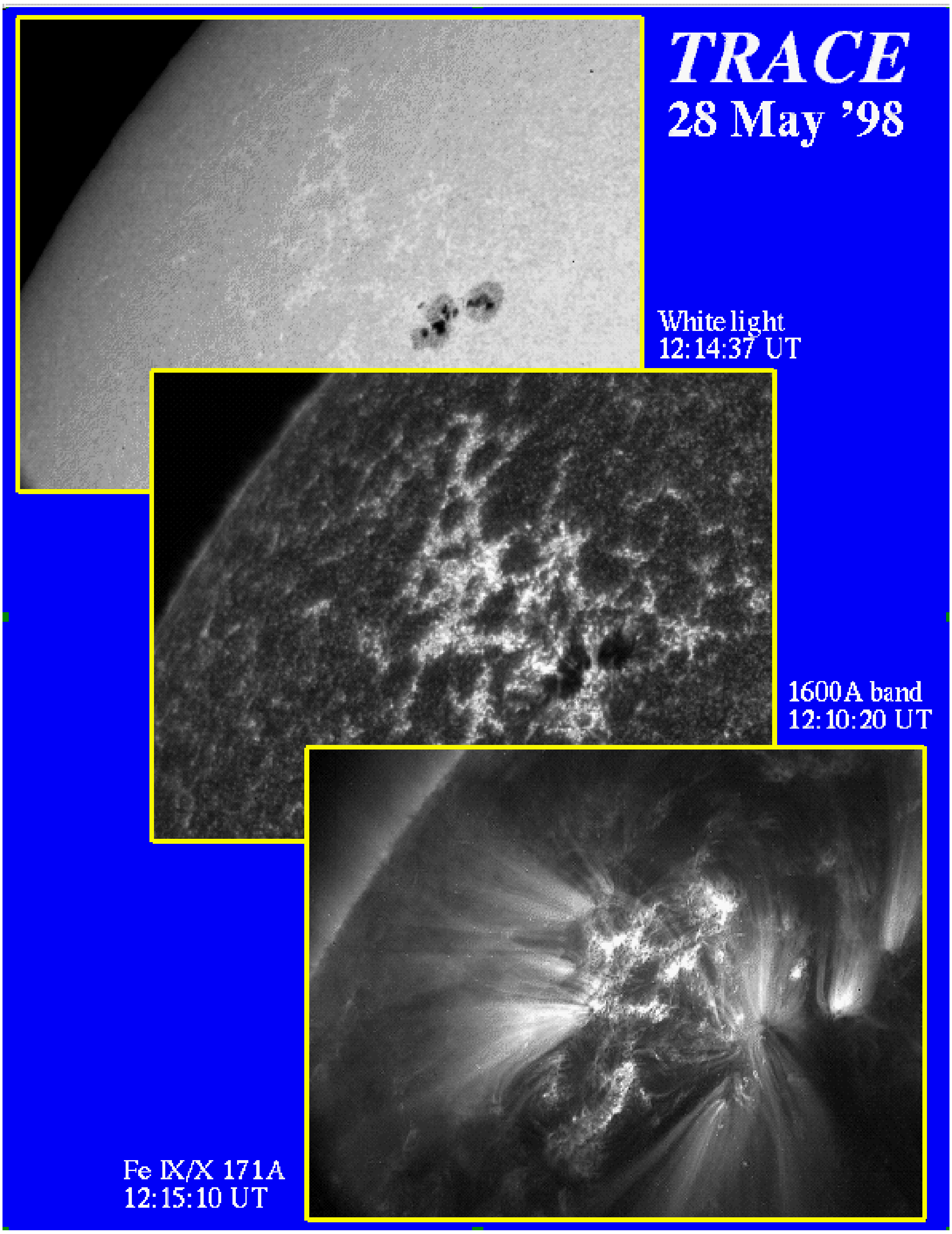

Figure 1.1: Solar features observed at three different wavelengths, at three different heights and temperatures: solar photosphere in white light (temperature 4000–6000 K), chromosphere at 1600 Å (4000–10 000 K), and corona in the Fe IX/X iron line temperature (160 000 – 2 million K). Sunspots are best observed at photospheric level, dark *umbra* in the middle and lighter *penumbra* surrounding it. Chromospheric images show fine structures and features connected with the magnetic network. In the corona magnetic loops are visible due to hot plasma flows. (TRACE satellite images)

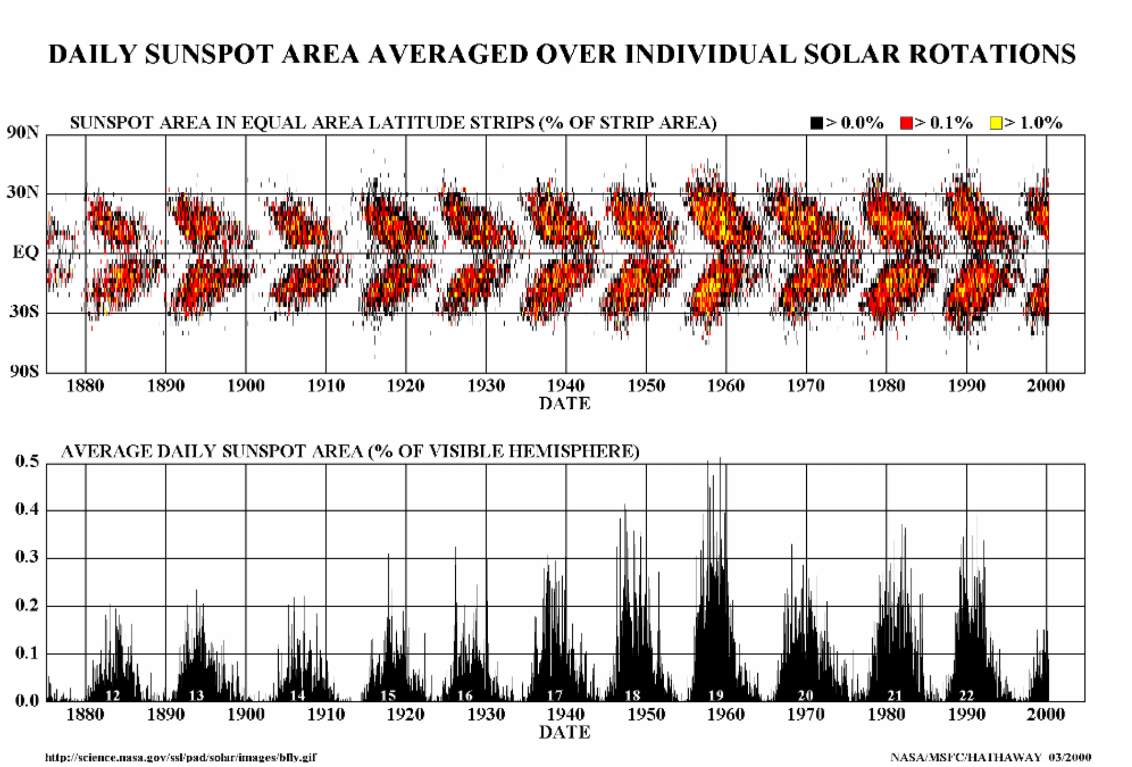

Figure 1.2: Sunspot cycles have been observed since the 1650's. The average length of one cycle is about 11 years. However, the length has been observed to vary between 9 and 14 years. 'New' sunspots, at the beginning of each cycle, are observed first at high solar latitudes. As the cycle progresses, sunspots appear closer to the solar equator. This is usually illustrated with a *butterfly diagram*. The number of sunspots and the total area covered by sunspots also show a similar cycle.

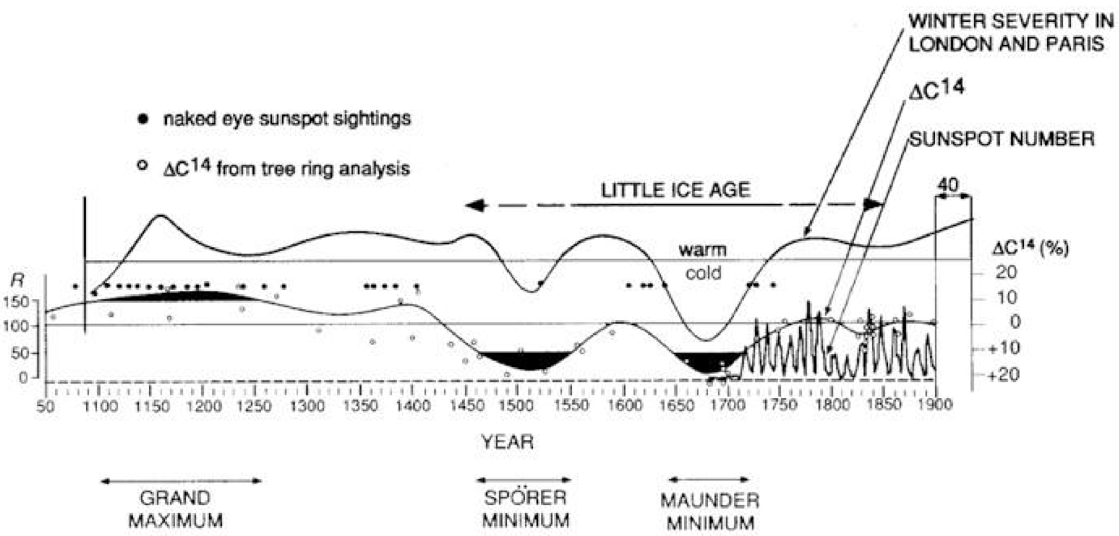

Figure 1.3: Sunspot cycles have shown so-called grand minimums, when sunspots numbers have been very low. The best-known is the Maunder minimum (1645 – 1715) which co-incided with a lengthy cold spell, 'the Little Ice Age'. Radio-carbon record from tree-ring samples show an increased amount of ^{14}C isotope during that time. It is believed that during low solar activity the impact of cosmic radiation increases (the 'shield' of sun-earth connection is missing).

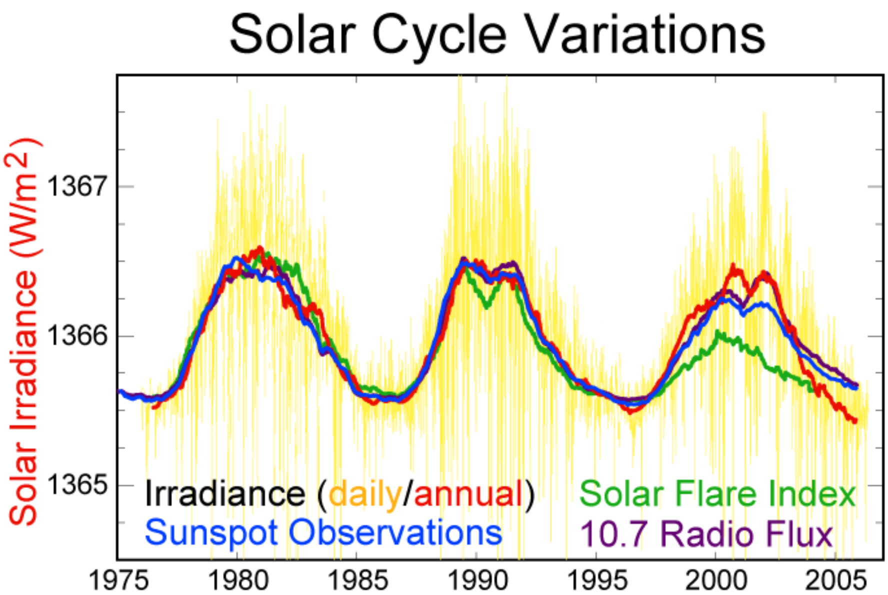

Figure 1.4: Solar activity can be monitored several different ways. In addition to daily sunspot numbers, solar irradiance, number of solar flares, and changes in the radio flux density at microwaves reflect the 11 year activity cycle. The so-called 'solar constant' is 1.37 kW/m^2 on average, but the cycle variation is visible also here. The 'constant' describes the solar radiation that falls on an area above the atmosphere at a vertical angle; on earth it varies with the time of day and year as well as with the latitude and weather. (Image courtesy of Wikipedia, Robert A. Rohde, Global Warming Art project)

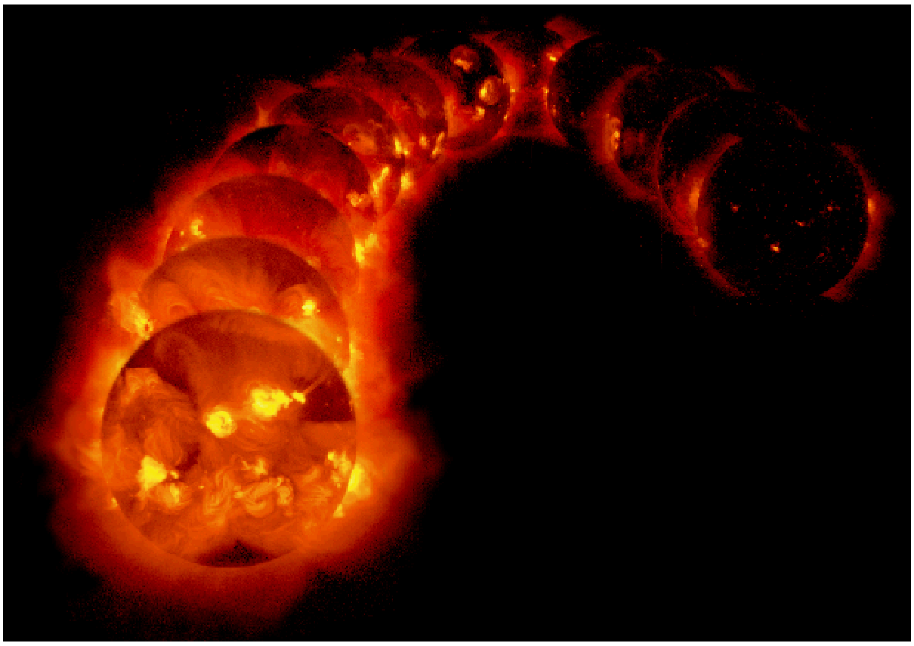

Figure 1.5: The changes in solar activity are well-observed also in soft X-ray images. During activity minimum, only a few bright points and some simple, isolated active regions are visible. During activity maximum the sun is covered with complex, multipolar active regions, and plasma flows along large-scale loops make the sun appear bright also high in the solar corona. (Image courtesy of Yohkoh SXT)

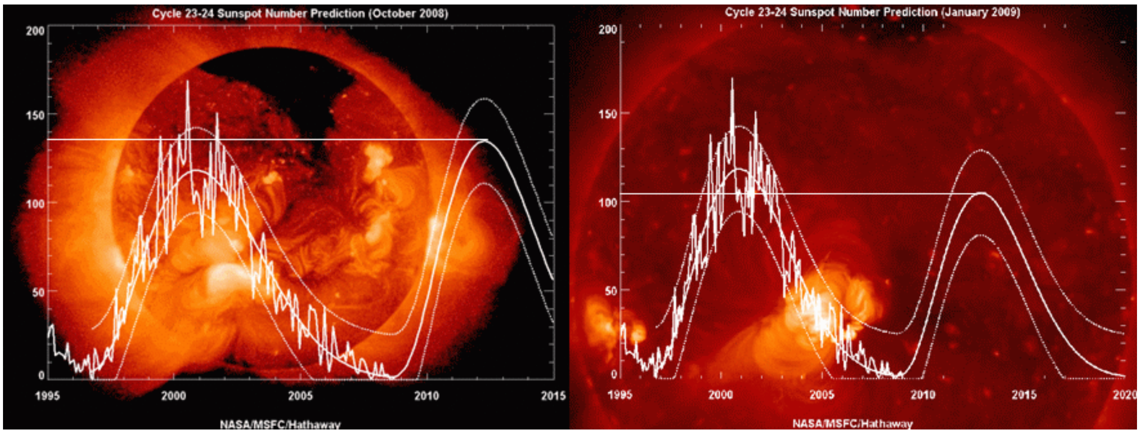

Figure 1.6: Solar cycle predictions by NASA's David Hathaway, in October 2008 and updated in January 2009. For the new solar cycle 24, the prediction for the number of sunspots has gone down quite a lot: Hathaway's predicted maximum in March 2006 was 145, in October 2008 it was 137, and in January 2009 it was 104. Also, the start of the new cycle was delayed. (image courtesy of http://www.klimadebat.dk/forum/attachments/).

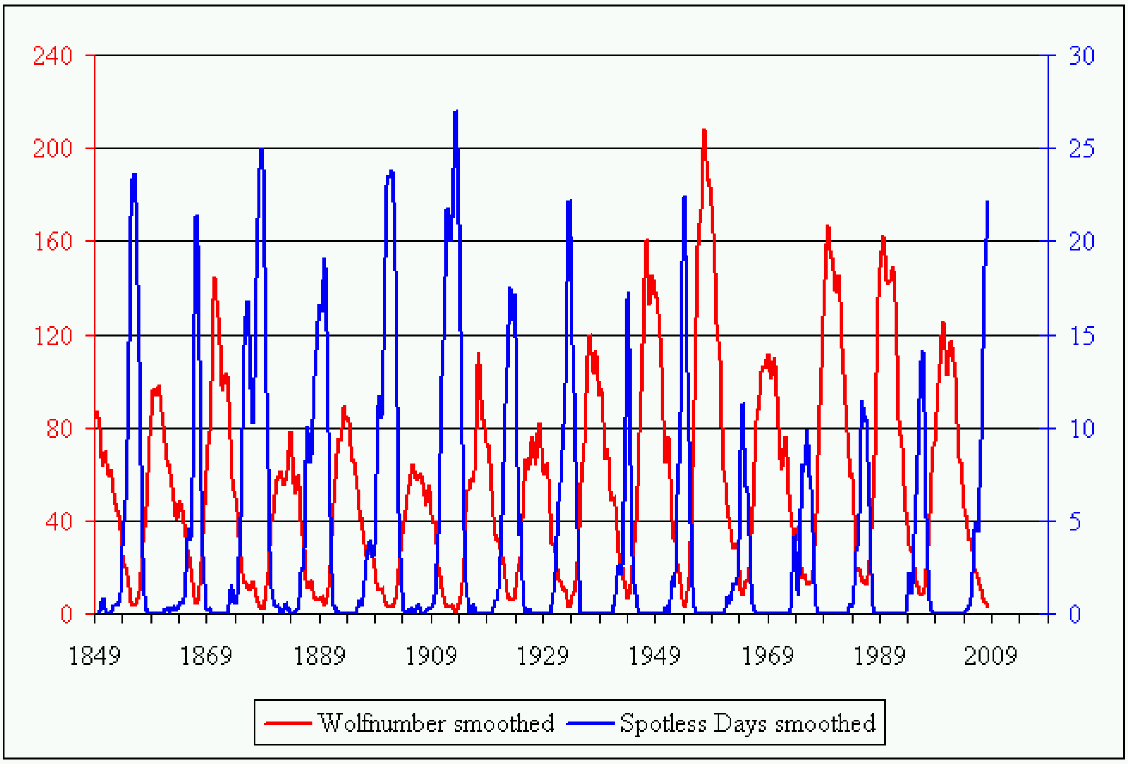

Figure 1.7: The graph shows the smoothed monthly Wolf number (red) and smoothed monthly number of spotless days (blue) since 1849. The current Wolf number is already at 2,9 and still decreasing, implying high smoothed number of spotless days of around 25. This is comparable with the low activity transits in the early 20th-century, and certainly contrasts with the previous 4 cycle transits. (Image and text courtesy of Solaemon's Spotless Days Page, at http://users.telenet.be/j.janssens/Spotless/Spotless.html)

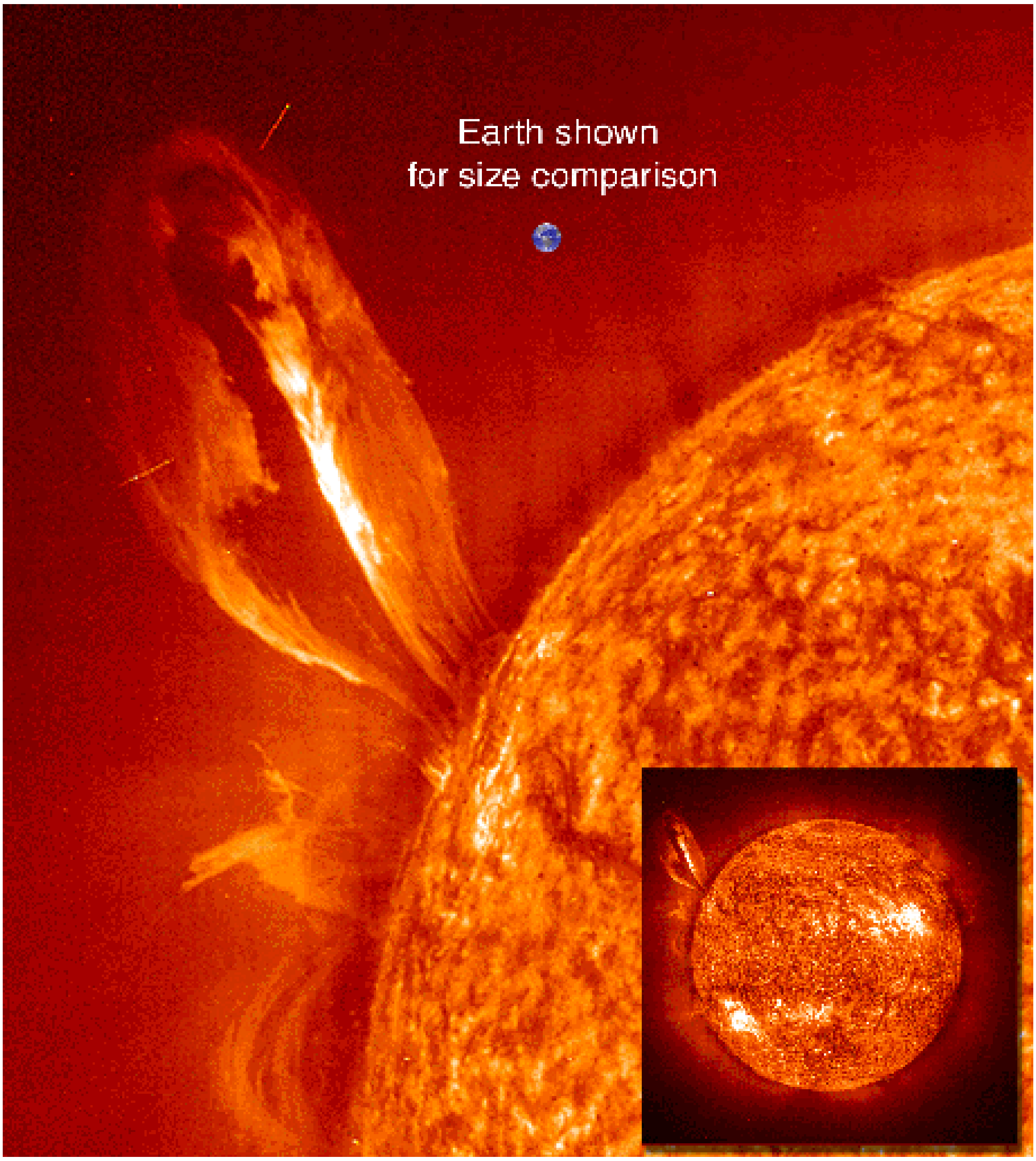

Figure 1.8: SOHO EIT image at He II (304 Å) wavelength, showing a large loop-like prominence located over the solar limb. The temperature range in this EUV image is approximately 60 000 – 80 000 K. The spatial resolution of EIT is 2.6 arc sec; one arc sec on the sun corresponds to about 700 km.